Clinical Neurophysiology 110 (1999) 1585–1588

# Neural source estimation from a time–frequency component of somatic evoked high-frequency magnetic oscillations to posterior tibial nerve stimulation

Kenji Sakuma[a,*], Kensuke Sekihara[b], Isao Hashimoto[a, c]

[a]*Department of Integrative Physiology, National Institute for Physiological Sciences, Okazaki 444-8585, Japan*
[b]*JST Mind Articulation Project, Yushima 4-9-2, Bunkyo, Tokyo 113-0034, Japan*
[c]*Department of Psychophysiology, Tokyo Institute of Psychiatry, 2-1-8 Kasmikitazawa, Setagaya-ku, Tokyo 156-0057, Japan*

Accepted 15 April 1999

**Abstract**

**Objective**: High frequency oscillations (HFOs) evoked by posterior tibial nerve stimulation were recorded using magnetoencephalography (MEG). Time–frequency domain multiple signal classification (TF-MUSIC) algorithm was applied, and the usefulness of this method was demonstrated.

**Methods**: Ten normal subjects were studied. To localize sources for the HFOs of those somatosensory evoked fields, we applied two kinds of methods: the single moving dipole (SMD) method and the TF-MUSIC method. The SMD method was applied after digitally band-pass filtering the somatosensory response with a bandwidth of 500–800 Hz. To estimate the locations of sources with the TF-MUSIC algorithm, we first set the target region on the spectrogram of the somatosensory responses. Then, the procedure described in Section 2.2 was applied with this target region.

**Results**: A clear, isolated region was detected in 6 out of 10 subjects using a time–frequency spectrogram. The averaged distance of the dipole sources between the HFOs and the underlying P37m using the TF-MUSIC algorithm was smaller than using the SMD method.

**Conclusions**: The TF-MUSIC algorithm is suitable for extracting a target response whose spectrum changes significantly during the observation. 

*Keywords:* Somatosensory cortex; High-frequency magnetic oscillations; Posterior tibial nerve; Magnetoencephalography; Time–frequency components; Multiple signal classification algorithm

## 1. Introduction

High-frequency primary cortical oscillations characterized by a frequency range of 500–800 Hz superimposed on the ascending slope of the N20 primary response following stimulation of the median nerve have been reported previously (Yamada et al., 1988; Curio et al., 1994; Hashimoto et al., 1996). We recorded high frequency oscillations (HFOs) evoked by posterior tibial nerve stimulation using magnetoencephalography (MEG), and demonstrated the intracranial locations of the HFOs sources with respect to brain anatomy (Sakuma and Hashimoto, 1999). Since the HFOs are of extremely low amplitude with low signal-to-noise ratio (S/N) compared with the underlying P37m, it was difficult to estimate the location of HFOs source precisely. We applied a time–frequency multiple signal classification (TF-MUSIC) algorithm to HFOs, and could demonstrate the superiority of this method compared to a single moving dipole solution method (SMD).

## 2. Materials and methods

Ten normal subjects (5 females and 5 males; mean age 26.6 years, range 21–35 years) were studied. They gave their consent to the experimental procedures. Electrical stimuli with 0.2 ms duration were delivered to the right posterior tibial nerve at the ankle (cathode proximal). The stimulus intensity was about 3 times the sensory threshold and elicited a mild twitch of toe. The stimuli were delivered at regular intervals with a repetition rate of 4 Hz. Magnetic recordings (bandpass 0.1–1200 Hz) were taken from the vertex centering around the Cz of the international 10-20 system with a 37-channel biomagnetometer (Magnes,

* Corresponding author. Tel.: + 81-564-55-7768/7766; fax: + 81-564-52-7913.

*E-mail address:* sakuma@nips.ac.jp (K. Sakuma)

1388-2457/99/$ - see front matter  CLINPH 98179
PII: S1388-2457(99)00120-0

Biomagnetic Technologies Inc., San Diego, CA) in a magnetically shielded room.

An epoch of 60 ms duration (10 ms pre- and 50 ms post-stimulus) was digitized at a 4167 Hz/channel sampling rate and 9999 responses were averaged off-line. DC offset was based on the pre-stimulus period. A local spherical model was fitted to the digitized head shape over the recording area for each subject.

### 2.1. SMD method

For separation of the HFOs from the underlying P37m, the wide-band (0.1–1200 Hz) recorded responses were digitally filtered with a 500–800 Hz band-pass filter. The location, orientation, and amplitude parameters of a dipole source model in the spherical head model were iteratively adjusted to obtain the least-squares error fit between an observed field and a theoretical field produced by the dipole source model (Sarvas, 1987). The correlation between the theoretical field generated by the model and the observed field was calculated and only equivalent current dipoles (ECDs) with a correlation above 0.86 were analyzed.

### 2.2. TF-MUSIC algorithm

The time–frequency MUSIC algorithm allows us to estimate the locations of neural sources from any time–frequency region of interest (Sekihara et al., 1998a, b). In this algorithm, we first calculate $\boldsymbol{C}_b(t,f)$, the time–frequency representation matrix for the measured data. Its diagonal elements are the auto-time–frequency distributions of the channel recordings and its off-diagonal elements are the cross-time-frequency distributions between different channel recordings. The matrix $\boldsymbol{C}_b(t, f)$ can be calculated using both linear and quadratic time–frequency representations. Let us define the time–frequency representation matrix for the source activities as $\boldsymbol{C}_s(t,f)$. Its diagonal elements are the auto-time–frequency distributions of the source activities and its off-diagonal elements are the cross-time–frequency distributions between different source activities.

Let us also define the matrices $\boldsymbol{Y}_b$ and $\boldsymbol{Y}_s$ as those obtained by averaging $\boldsymbol{C}_b(t, f)$ and $\boldsymbol{C}_s(t, f)$ over the target time–frequency region $\Omega$ for which the neural sources are localized; i.e. $\boldsymbol{Y}_b = \iint_\Omega \boldsymbol{C}_b(t,f)\,dt\,df$ and $\boldsymbol{Y}_s = \iint_\Omega \boldsymbol{C}_s(t,f)\,dt\,df$, where $\iint_\Omega$ indicates the integral over the target time–frequency region. Assuming that the noise and signal are uncorrelated in the target region and the noise is white Gaussian, we finally derive the relationship

$$\boldsymbol{Y}_b = (\boldsymbol{L}_c)\boldsymbol{Y}_s(\boldsymbol{L}_c^T) + \rho^2\boldsymbol{I} \tag{1}$$

where $\boldsymbol{L}_c$ is the lead-field matrix for the true source locations, $\rho^2$ is the total noise power in the target region and $\boldsymbol{I}$ is the unit matrix.

Let us denote the noise-level eigenvectors of $\boldsymbol{Y}_b$ as $\boldsymbol{u}_j$ $(j = P_\Omega + 1,\ldots, M)$. Here $P_\Omega$ is the number of sources whose activities have time–frequency components in the target region. Therefore, when the matrix $\boldsymbol{Y}_s$ is a full-rank matrix, Eq. (1) leads to

$$\boldsymbol{L}_c^T u_j = 0 \qquad for \qquad j = P_\Omega + \mathbf{1},\ldots,\boldsymbol{M} \tag{2}$$

This equation indicates that source locations can be obtained by checking the orthogonality between the sensor lead field $\boldsymbol{L}(\boldsymbol{x})$ and the noise-level eigenvectors of $\boldsymbol{Y}_b$. This orthogonality can be evaluated by calculating the following localizing function,

$$J(x) = 1/\lambda_{\min}\left[L(x)^T Z_N Z_N^T L(x), L(x)^T L(x)\right] \tag{3}$$

where the matrix $\boldsymbol{Z}_N$ is defined as $\boldsymbol{Z}_N = [\boldsymbol{u}_{P_\Omega}+1,\ldots, \boldsymbol{u}_M]$ and $\lambda_{\min}[.,.]$ indicates the generalized minimum eigenvalue of the matrix pair given in parenthesis. Eq. (3) is calculated in a volume where sources can exist, and each location where $\boldsymbol{J}(\boldsymbol{x})$ reaches a peak is chosen as the location of one dipole source.

### 2.3. Evaluation of localization accuracy

The distances between ECD location of P37m and HFOs calculated with the SMD and between ECD location of P37m and HFOs calculated with TF-MUSIC were compared and the accuracy of ECD location between the two methods were assessed, since it is well established that the sources for HFOs and the underlying N20m for median nerve stimulation are very close to each other (Hashimoto et al., 1996). These distances were defined as $((x - x')^2 + (y - y')^2 + (z - z')^2)^{1/2}$, where $x$, $y$ and $z$ indicate P37m dipole locations and $x'$, $y'$ and $z'$, HFOs dipole location.

## 3. Results

In wide-band recordings, the main P37m deflection was clearly identified in all 10 subjects. The ECDs of P37m peak (SMD P37m) were estimated at the somatosensory foot area in all subjects. After filtering with a 500–800 Hz band-pass filter, low amplitude high-frequency magnetic oscillations superimposed on P37m were detected in 5 out of 10 subjects. However, since the values of the correlation for the ECD sources of the HFOs were smaller than 0.86 in one subject, we calculated the ECDs of HFOs in only 4 subjects using the SMD method. With the SMD method, the ECD localizations for the high-frequency peaks and the underlying P37m were close with each other (Table 1). There were no significant statistical differences between the localizations for the $x$, $y$ and $z$ axes (paired $t$ test) (Table 1). The spectrogram was calculated for the frequency range above 400 Hz from the averaged wide-band somatosensory evoked magnetic fields (SEFs). The region containing the HFOs was selected as the target regions of interest. A clear and isolated time–frequency component was observable in 6 out of 10 subjects. The time–frequency region of interest started at 29–33 ms (30.8 ± 1.5ms) with 500–630 Hz (585 ± 44.6 Hz) in frequency, and ended at 35–40 ms (38.3 ± 1.8 ms)

Table 1
Individual source locations of P37m and HFOs and the distance between the locations of P37m and HFOs using the SMD and TF-MUSIC alogorithm[a]

| Subject | SMD P37m | | | SMD HFOs | | | TF-MUSIC HFOs | | | Distance (cm) | |
|---|---|---|---|---|---|---|---|---|---|---|---|
| | $x$ | $y$ | $z$ | $x$ | $y$ | $z$ | $x$ | $y$ | $z$ | SMD | TF-MUSIC |
| KT | 1.52 | 1.41 | 10.25 | N.E. | N.E. | N.E. | 0.80 | 1.57 | 10.14 | N.E. | 0.74 |
| MK | 1.09 | 1.89 | 10.29 | 1.03 | 2.41 | 9.44 | − 0.46 | 1.52 | 10.40 | 1.00 | 1.59 |
| YI | 0.90 | 1.35 | 10.73 | 0.68 | 1.36 | 10.33 | 1.65 | 2.26 | 10.50 | 0.46 | 1.20 |
| KS | 1.92 | 1.19 | 10.66 | 1.25 | 2.54 | 10.31 | 3.11 | 1.95 | 9.57 | 1.55 | 1.78 |
| AG | −0.22 | 1.27 | 10.23 | N.E. | N.E. | N.E. | 0.49 | 2.22 | 10.02 | N.E. | 1.21 |
| TO | 0.17 | 1.36 | 10.95 | −0.27 | 0.54 | 9.54 | 0.18 | 1.38 | 10.65 | 1.70 | 0.30 |
| Average | | | | | | | | | | 1.17 | 1.14 |
| SD | | | | | | | | | | 0.57 | 0.55 |

[a] Comparison of values between SMD P37m and SMD HFOs, not significant. Comparison of values between SMD P37m and TF-MUSIC HFOs, not significant. Comparison of values between Distance SMD and Distance TF-MUSIC, not significant. N.E., not estimated.

with 650–800 Hz (725 ± 50.1 Hz) in frequency. These time ranges were coincident with the ascending and descending slopes of the P37m. Fig. 1A shows a typical record from one subject where the ECDs of HFOs could be estimated by using both the SMD and the TF-MUSIC. Fig. 1B shows a typical result from another subject showing clear isolated region in the time–frequency spectrogram although the SMD algorithm failed to estimate the ECD localization due to a low signal-to-noise ratio with a low correlation value. We then applied the TF-MUSIC algorithm to these target regions. Typical TF-MUSIC localizing function maps are shown in Fig. 2. The contours in this figure show the relative values of the TF-MUSIC localization function (Eq. (3)) projected onto the transverse, coronal and sagittal planes. Although the average distance of the dipole sources between the HFOs and the underlying P37m was not significantly different between SMD method and TF-MUSIC algorithm, it should be noted that HFO dipole locations were estimated in 6 out of 10 subjects with the TF-MUSIC algorithm as against in 4 out of 10 subjects with the SMD method (Table 1).

## 4. Discussion

In this study, the TF-MUSIC algorithm was applied to estimating the neural sources of the high-frequency magnetic oscillations evoked by posterior tibial nerve stimulation. The dipole locations of the HFOs were successfully estimated using the TF-MUSIC algorithm even when the estimations failed with the SMD method. This is mainly because only the high-frequency oscillatory activities visualized in a time–frequency spectrogram were used for calculation. The dipole strength of the HFOs is as small as one

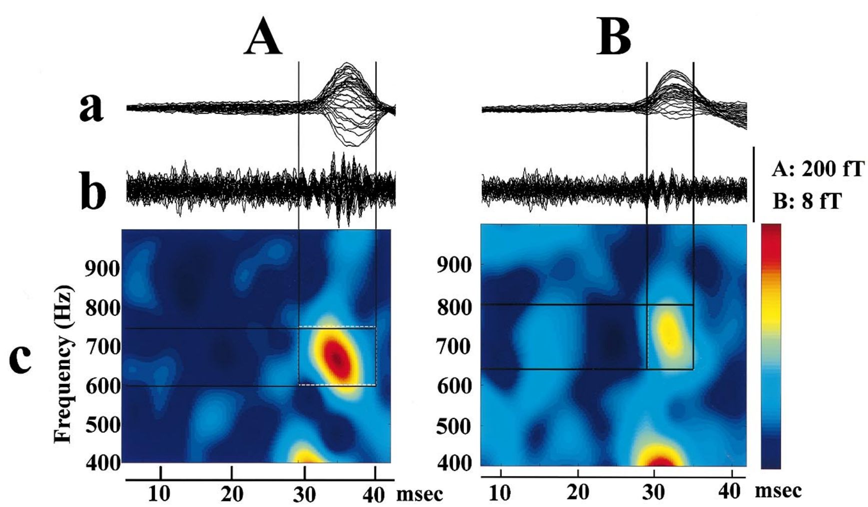


Fig. 1. (A) A typical recording from one subject where the ECD of HFOs could be estimated using both the SMD algorithm and the TF-MUSIC algorithm (subject TO). Wide-band recorded somatosensory evoked magnetic fields following right posterior tibial nerve stimulation. Thirty-seven waveforms are superimposed to illustrate the polarity-reversed P37m deflections (a). High-frequency oscillations after digital filtering (500–800 Hz) the wide-band somatosensory magnetic fields illustrated in (a). The high-frequency oscillations are roughly coincident with the P37m (b). Averaged spectrogram for the frequency range above 400 Hz obtained from the MEG data is shown in (c). A rectangle with a dotted line is the target region for the HFOs. (B) A typical result from another subject showing a clear isolated region in time–frequency spectrogram although the ECD of HFOs could not be estimated with the SMD algorithm due to a low signal-to-noise ratio with a low correlation value (correlation = 0.74) (subject AG).

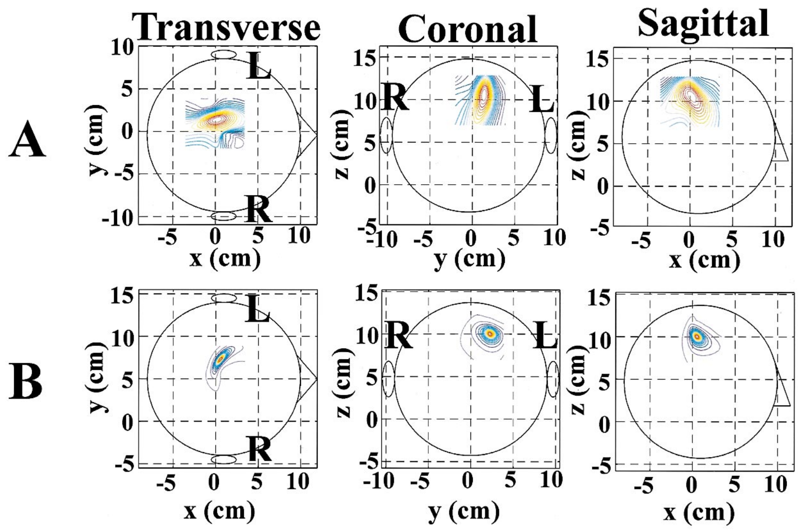


Fig. 2. (A,B) TF-MUSIC localization function projected onto transverse, coronal and sagittal planes with the target region chosen in Fig. 1A and B, respectively.

fourteenth of the N20m for median nerve stimulation (Hashimoto et al., 1996). In addition, it is widely known that somatosensory evoked potentials evoked by posterior tibial nerve stimulation are more difficult to record than those evoked by median nerve stimulation. Although we used 'massive' averaging over nearly 10 000 stimulus presentations to obtain the desirable S/N, it is impossible to eliminate all magnetic noise such as external ambient noise, system noise and brain noise. Since such a magnetic noise has no phase-locking to the stimulus, the clear isolated activity detected in the averaged time–frequency spectrogram should be the signal free from the noise. In fact, the TF-MUSIC has theoretical as well as empirical advantages for eliminating noise from the evoked magnetic fields (Sekihara et al., 1998a,b). With this algorithm, the time–frequency spectrogram of evoked magnetic response can be checked by visual inspection for inclusion in the analysis. Therefore, the TF-MUSIC algorithm is suitable for extracting a target response whose spectrum changes significantly during the observation.

## References

Curio G, Mackert BM, Burghoff M, Koetitz R, Abraham-Fuchs K, Harer W. Localization of evoked neuromagnetic 600 Hz activity in the cerebral somatosensory system. Electroenceph clin Neurophysiol 1994;91:483–487.

Hashimoto I, Mashiko T, Imada T. Somatic evoked high-frequency magnetic oscillations reflect activity of inhibitory interneurons in the human somatosensory cortex. Electroenceph clin Neurophysiol 1996;100:189–203.

Sakuma K, Hashimoto I. High-frequency magnetic oscillations evoked by posterior tibial nerve stimulation. NeuroReport 1999;:2.

Sarvas J. Basic mathematical and electromagnetic concepts of the biomagnetic inverse problem. Phys Med Biol 1987;32:11–22.

Sekihara K, Nagarajan S, Poeppel D, Miyauchi S, Takino R, Fujimaki N, Miyashita Y. Estimating neural sources from each time–frequency component of MEG data. Neuroimage 1998a;7:S673.

Sekihara K, Nagarajan S, Poeppel D, Miyashita Y. Time–frequency MEG-MUSIC algorithm. IEEE Trans Med Imaging 1998b; in press.

Yamada T, Kameyama S, Fuchigami Y, Nakazumi Y, Dickins QS, Kimura J. Changes of short latency somatosensory evoked potential in sleep. Electroenceph clin Neurophysiol 1988;70:126–136.